Decrease in Solvent Evaporation Rate Due to Phase Separation in Polymer Films

Masato Yamamura, Kouhei Horiuchi, Toshihisa Kajiwara, and Kitaro Adachi
Dept. of Applied Chemistry, Kyushu Institute of Technology, Fukuoka, 804-8550, Japan

The removal of volatile solvents from polymeric films is of technological importance for producing composite materials such as functional coatings. For "miscible" fluids, successful physical models have been presented to predict the solvent removal rate by considering two rate-limiting processes: the convective diffusion in the bounding gas phase, and the molecular diffusion in the multicomponent liquid (Okazaki et al., 1974; Cairncross et al., 1995; Alsoy and Duda, 1999). In the former, a partial pressure difference between the liquid–gas interface and the gas far from the interface provides a driving force for the solvent transport, which depends on the vapor–liquid equilibria at the interface. In contrast, the latter process dominates the evaporation in concentrated solutions because a strong interaction between the solvent and polymers causes diffusion coefficients to be decreased by orders of magnitude in polymeric fluids (Zielinski and Duda, 1992), resulting in diffusion-limited evaporations.

However, few physical models are currently available for describing solvent evaporation in "immiscible" polymer blends. Because the solvent evaporation can quench the blend into a particular location in the two-phase region, we expect that the resulting phase separation will vary the vapor–liquid equilibria and/or the diffusion coefficients in the demixed phases, leading to different evaporation behaviors from those in nonseparating fluids. The major difficulty in understanding the solvent evaporation in immiscible blends stems from the fact that the domain grows in a nonequilibrium state, in which various physical properties depend upon the polymer compositions in each separating phase and would vary with time in a complicated manner. To date, most theoretical studies assume that the dynamics of solvent evaporation in thermodynamically unstable blends is the same as that in homogenous stable solutions (Shojaie et al., 1994; Matsuyama et al., 1997). In contrast to the extensive studies on the dynamics of microstructure evolutions in polymeric liquids, the validity of this assumption has not yet been verified. The objective of this article is to demonstrate the first quantitative evidence that the solvent evaporation rate decreases due to phase separation in a particular range of solvent contents.

Correspondence concerning this article should be addressed to M. Yamamura.

Experimental Procedures

The polymer blends used in this study contained polystyrene (PS, Wako Chemical, $Mn = 115{,}000$, $Mw/Mn = 1.8$) and polycarbonate (PC, Mitsubishi Chemical, $Mn = 32{,}400$, $Mw/Mn = 1.8$), where Mn and Mw are the number average and weight average molecular weights, respectively. Both polymers are dissolved in tetrahydrofuran (THF, Wako Chemical, as purchased) as the common solvent. The weight ratio of PS/PC/THF was 1:1:105. The initial solution was homogenous and optically clear. The solution was deposited on a 0.10-m × 0.025-m aluminum substrate mounted on an electronic balance (Sartorius, LP620). The film was dried in a 0.10-m × 0.15-m × 1.2-m plastic duct in which air flowed parallel to the sample at a constant temperature of $T = 30.5$°C. The mass of the film during drying was measured by the electronic balance and stored in a personal computer to calculate the drying rate, $r = -(1/A)(dW/dt)$ as a function of the solvent content $\omega = (W - W_0)/W_0$, where A is the surface area of the film, t the time, W the mass of the film, and W_0 the final mass of the film after drying. Because the mass measurement was often disturbed by a fluctuation in the air flow, an average of five neighboring data points was taken as a smoothed W value at each time and used in the calculations. Top views of the phase morphology of the dried film were obtained using an optical microscope and were stored as photographic images. A toluene etching technique was used to distinguish the polystyrene and polycarbonate phases in the film. The PS-rich phase can be removed by immersion in toluene because toluene is a selective solvent for polystyrene.

Results and Discussion

First, we demonstrated the transition in the microstructure evolutions by variations in the evaporative conditions. Top views of the final phase morphology for three different air velocities are shown in Figures 1a–1c. The initial and final film thicknesses were 800 μm and 15 μm, respectively. It was found that an increase in air velocity results in a transition of the phase morphology from a random distribution of droplets (Figure 1a) to periodic stripe patterns whose axes are aligned in the air-flow direction (Figure 1c). Microscope observations of the top and bottom film surfaces revealed that the peri-

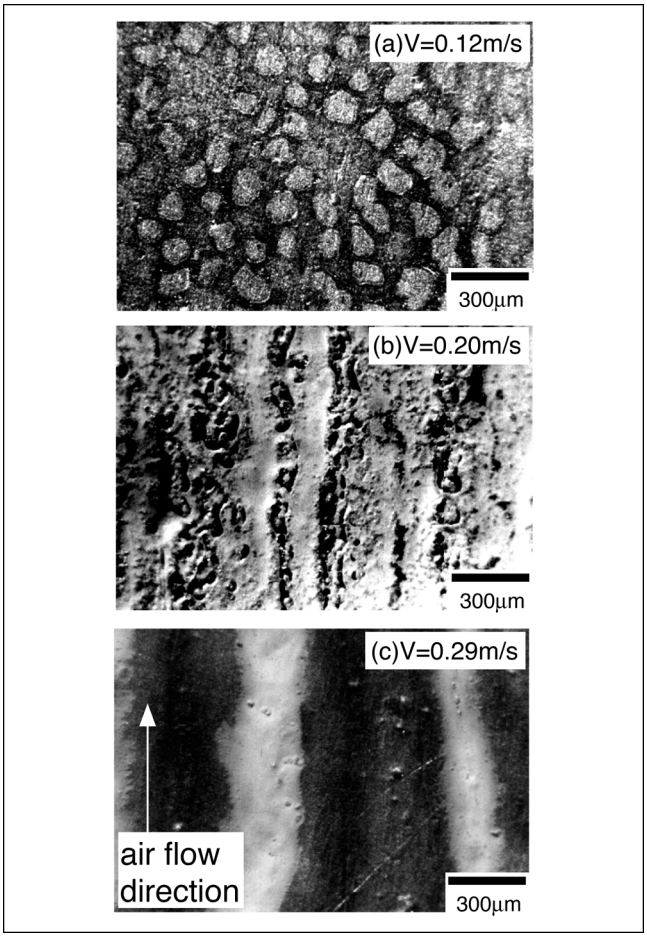

Figure 1. Effect of air velocity on final domain structures in evaporated film.

The initial film thickness was 800 μm. The film exhibits a transition in domain morphology from a random distribution of droplets to periodic stripe patterns.

odic stripes developed not only on the top surface but also across the film. Toluene etching showed that the white stripe phases in the figure were polycarbonate-rich phases, which remained after the immersion of the sample in toluene. The coalescence of the PC-rich droplets into an elongated phase was observed at the intermediate velocity of 0.20 m/s (Figure 1b).

In the second series of experiments, the initial film thickness of the liquid films was varied, while the air velocity was kept constant. Figures 2a–2d show the final phase morphologies for four different initial film thicknesses. With decreasing initial film thickness, the widths of the stripe patterns decrease (Figure 2b), break into pieces (Figure 2c), and eventually disappear at the initial thickness of 200 μm (Figure 2d). The decrease in stripe width is accompanied by an increase in the number density of the stripe patterns.

The ordered stripe pattern formation can be understood in terms of the coupling between the surface-tension-driven flows and the microstructure development via phase separation. It has been demonstrated that the Bénard–Marangoni convection can become a source of ordered patterns in polymeric fluids (Mitov and Kumacheva, 1998). In our experiments, preliminary visualizations of the evaporating films showed a development of stripelike convections consisting of pairs of counterrotating rolls that flow from the downstream area to the upstream area in a spiral motion. For a nonevaporating fluid, the theoretical stability analysis has demonstrated that a temperature variation imposed along the surface induces stationary longitudinal rolls whose axes are aligned in a direction parallel to the temperature gradient (Smith and Davis, 1983). Such a temperature gradient along the surface formed in our evaporating coatings because the hot airflow caused the fluid to be evaporated more rapidly in the upstream area than in the downstream area, leading to a cooler surface temperature in the upstream area. The temperature variation in the air-flow direction can induce a surface-tension distribution along the interface, which drives a flow along the surface from the lower surface-tension region in the downstream area to the higher surface-tension region in the upstream area. The surface-tension-driven flow possibly enhances the droplet coalescence in the longitudinal rolls aligned in the direction parallel to the airflow and leaves the periodic stripe patterns in that direction after the film dries. For a small airflow in Figure 1a, the temperature gradient along the free surface is so small that the interaction between the convection and the phase separation becomes too weak to induce the stripe patterns.

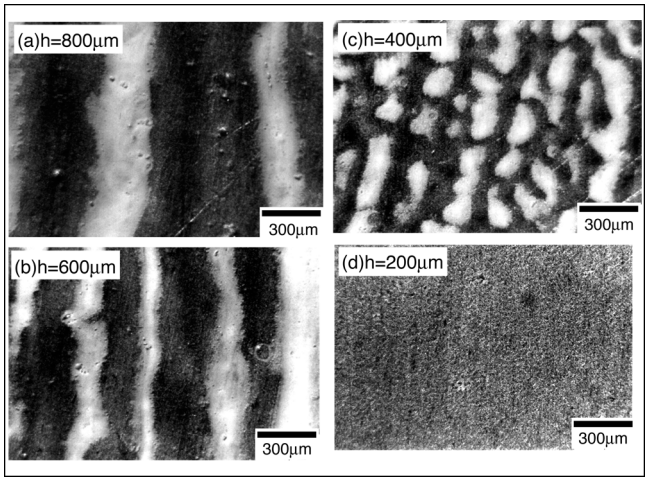

Figure 2. Effect of initial film thickness on final domain structures in evaporated film.

Air velocity was 0.29 m/s. Decreasing film thickness breaks the periodic stripes into separated domains.

The coupling between the convection and the phase separation was also verified by the fact that the stripe width decreases with decreasing film thickness (Figures 2a–2d). The surface-tension-driven convection can be stabilized in thin films due to viscous and thermal dissipations. A larger viscous friction can act on a thinner film confined between the solid substrate and the free surface. At the same time, the decrease in film thickness leads to an increase in conductive heat flux, which dissipates the surface-tension variations at the free surface and suppresses the liquid motion. The stabilized convection no longer couples with the phase separation, and, hence, induces homogenous phases in spite of the stripe patterns.

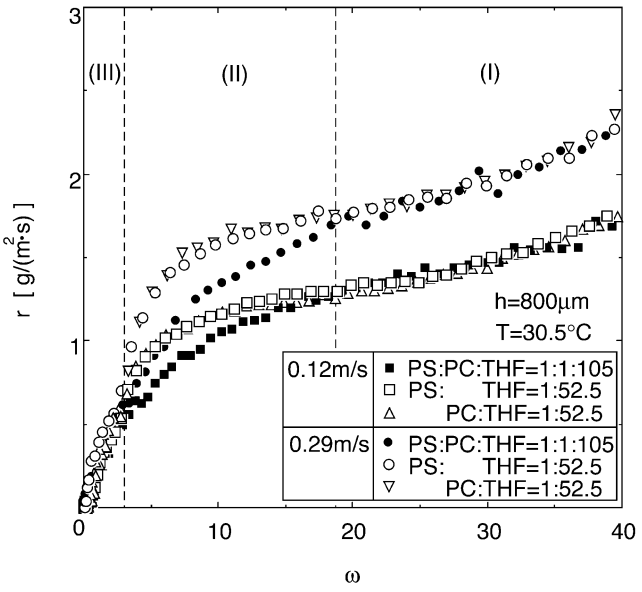

Figure 3. Effect of air velocity on solvent evaporation rate.

The drying-rate curves are presented in terms of solvent content, that is, the weight ratio of the solvent to the polymers. The closed symbols denote the evaporation rates in the ternary solutions at air velocities of 0.12 m/s (square) and 0.29 m/s (circle), respectively. The open symbols denote the evaporation rates in the binary solutions at air velocities of 0.12 m/s (square: PS/THF system, triangle: PC/THF system) and 0.29 m/s (circle: PS/THF system, triangle: PC/THF system). The ternary solutions exhibit lower evaporation rates than the binary solutions in Regime II.

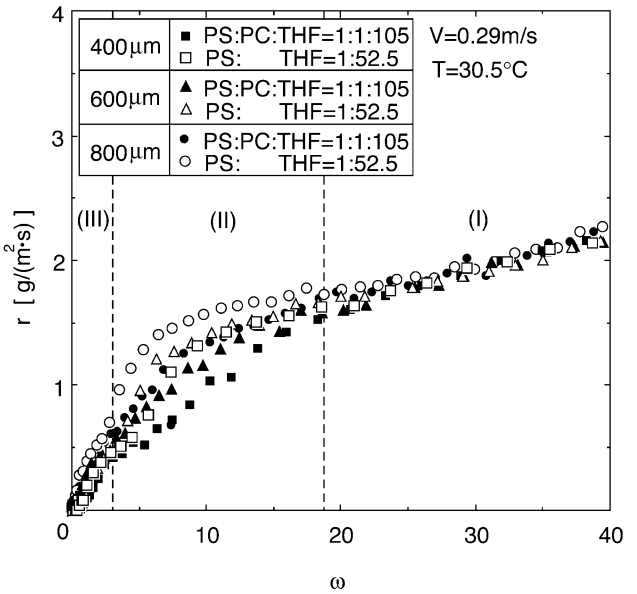

Figure 4. Effect of initial film thickness on solvent evaporation rate.

The drying rate curves are presented in terms of solvent content ω. The closed symbols denote the evaporation rates in the ternary solutions at the initial film thickness of 400 μm (square), 600 μm (triangle), and 800 μm (circle). The open symbols denote the evaporation rates in polystyrene/THF binary solutions.

Next, we show one of the most extreme cases in order to demonstrate how the microstructure evolution affects the solvent evaporation rate. Figure 3 shows the measured evaporation rates at two different air velocities, V, of 0.12 m/s and 0.29 m/s, corresponding to the drying conditions shown in Figures 1a and 1c, respectively. The drying rate curves are presented in terms of the solvent content ω, that is, the weight ratio of the solvent to the polymers. Open and closed symbols in the figure represent the evaporation rates in the polystyrene/THF and polycarbonate/THF binary solutions exhibiting no phase-separated structure, and those in the ternary solutions with the droplets or the stripe pattern formation. At high solvent contents (Regime I), the evaporation rates in the ternary solution agree well with those in the binary solutions. With decreasing solvent content (Regime II), it was found that the ternary solutions exhibited lower evaporation rates than the homogenous binary solutions. The decrease in evaporation rate was observed for both air velocities in spite of the drastic morphology change from the droplet phase to the stripe patterns. A further decrease in solvent content leads to a regime in which the evaporation rates rapidly fall and converge into a curve (Regime III). The transition from Regime I to Regime II occurs at the critical solvent content of $\omega_c = 18$. Cloud-point measurements indicated that the critical concentration, below which the phase separation could occur, was found to be $\omega = 17$, showing good agreement with ω_c. This result provided conclusive evidence that the evaporation rate decreases due to the microstructure development via phase separation.

In order to clarify the evaporation mechanism in Regimes I and II, the effect of the solvent evaporation rates on the initial film thickness, h, was measured for the ternary and binary systems. The solvent evaporation rates are shown in Figure 4 for three different initial film thicknesses that varied from 800 μm to 400 μm, corresponding to the morphology transition from the stripe patterns to the broken domains shown in Figures 2a–2c. The broken lines represent the boundaries between the regimes, in which the solution is homogenous (Regime I), phase separating (Regime II), and solidifying (Regime III), as described in Figure 3. It was found that the evaporation rates in Regime I depend upon neither the film thickness nor the polymer compositions. As the solvent content decreases into Regime II, the evaporation rate decreases with decreasing film thickness. The ternary solutions exhibit lower evaporation rates than the binary solutions, indicating the same behavior shown in Figure 3.

The independence of the evaporation rate on film thickness in Regime I implies that the evaporation is dominated by the convective diffusion in the bounding gas phase, and the vapor–liquid equilibrium at the polymer–gas interface is the key for the solvent transport. This is also consistent with the increase in evaporation rate with increasing air velocity (see Regime I in Figure 3). To evaluate the effect of the polymer concentration on the vapor–liquid equilibria, we estimated the saturated pressure of the polystyrene/tetrahydrofuran binary system using the Flory–Huggins theory. The ratio of the pressure in the binary solution p to that in the pure solvent p^0 was calculated assuming the interaction parameter between the polymer and solvent to be $\chi = 0.36$, which was obtained from the solubility data. The solvent content at which $p/p^0 = 0.9998$ holds was found to be $\omega = 18$ ($= \omega_c$).

This suggests that the saturated pressure at the interface is almost constant and agrees with that of pure solvent in Regime I. This is consistent with the fact that the evaporation rate was independent of polymer composition in Figures 3 and 4.

In contrast, the strong dependence of the evaporation rate on film thickness in Regime II indicates that the evaporation is limited by molecular diffusion in the liquid. This fact provides evidence that the decrease in evaporation rate in the ternary solution is due to the decrease in the molecular diffusion rates in the phase-separating phases rather than the decrease in saturated vapor pressure at the air/liquid interface. It is not immediately clear how the two immiscible polymers interact to reduce the diffusion coefficients in coexisting phases. Here we simply note that the diffusion coefficients in the phase-separating solutions could not be expressed as a simple combination of them in the nonseparating solutions. As found from Figure 3, the evaporation rates in the two binary solutions—the polystyrene/THF and polycarbonate/THF systems—agree well with each other in Regime II, indicating a similar diffusion mechanism between these two liquids. Direct measurements of the diffusion coefficients in the demixing solutions would provide us detailed physical descriptions of the mechanism of solvent transport in immiscible polymer blends, although few experimental data are currently available.

Conclusions

The solvent evaporation rate decreases due to the phase separation for a particular solvent-content range in immiscible polymer blends. The drying characteristics curve revealed three distinct evaporation regimes, corresponding to the transitions in the film structure and solvent-transport mechanism. The decrease in the evaporation rate was observed only in the intermediate regime, in which the evaporation is limited by the liquid diffusion. The increase in air velocity and film thickness induced a transition in the phase morphologies from the randomly distributed droplets to periodic stripe patterns. The decrease in evaporation rate was observed in all of these phase-separating films.

Acknowledgment

This work was supported in part by the Grant-in-Aid (No. 11750655) for Encouragement of Young Scientists from the Japan Society for the Promotion of Science.

Literature Cited

Alsoy, S., and J. L. Duda, "Modeling of Multicomponent Drying of Polymer Films," *AIChE J.*, **45**, 896 (1999).

Cairncross, R. A., S. Jeyadev, R. F. Dunham, K. Evans, L. F. Francis, and L. E. Scriven, "Modeling and Design of an Industrial Dryer with Convective and Radiant Heating," *J. Appl. Poly. Sci.*, **58**, 1279 (1995).

Matsuyama, H., M. Termoto, and T. Uesaka, "Membrane Formation and Structure Development by Dry-Cast Process," *J. Memb. Sci.*, **135**, 271 (1997).

Mitov, Z., and E. Kumacheva, "Convection-Induced Patterns in Phase-Separating Polymeric Fluids," *Phys. Rev. Lett.*, **81**, 3427 (1998).

Okazaki, M., K. Shioda, K. Masuda, and R. Toei, "Drying Mechanism of Coated Film of Polymer Solution," *J. Chem. Eng. Jp.*, **7**, 99 (1974).

Shojaie, S. S., W. B. Krantz, and A. R. Greenberg, "Dense Polymer Film and Membrane Formation via the Dry-Cast Process—Part I. Model Development," *J. Memb. Sci.*, **94**, 255 (1994).

Smith, M. K., and S. H. Davis, "Instabilities of Dynamic Thermocapillary Liquid Layers. Part 1. Convective Instabilities," *J. Fluid Mech.*, **132**, 119 (1983).

Zielinski, J. M., and J. L. Duda, "Predicting Polymer/Solvent Diffusion Coefficients Using Free-Volume Theory," *AIChE J.*, **38**, 405 (1992).

Manuscript received Nov. 13, 2001, and revision received Mar. 15, 2002.